# Thermal protection composites based on phenol-formaldehyde resin and reinforcing fibers

Meiirbekov M.N.

Sadykov M.Sh

Janikeyev M.S

Kuandyk A.B.

Yesbolov N.B.

See next page for additional authors

# Thermal protection composites based on phenol-formaldehyde resin and reinforcing fibers


## Authors

Meiirbekov M.N., Sadykov M.Sh, Janikeyev M.S, Kuandyk A.B., Yesbolov N.B., and Nurzhanov M.N

ORIGINAL STUDY

# Thermal Protection Composites Based on Phenol-formaldehyde Resin and Reinforcing Fibers

M.N. Meiirbekov [a], M.Sh. Sadykov [a,b,*], M.S. Janikeyev [a], A.B. Kuandyk [a,b], N.B. Yesbolov [a], M.N. Nurzhanov [a,c]

[a] JSC, National Center of Space Research and Technology, 1, Almaty 050010, Kazakhstan
[b] Faculty of Mechanics and Mathematics, Al-Farabi Kazakh National University, Almaty 050040, Kazakhstan
[c] School of Materials Science and Green Technologies, Kazakh-British Technical University, Almaty 050005, Kazakhstan

**Abstract**

**This study presents the development and experimental investigation of composite thermal insulation materials intended for application in solid-propellant rocket motors. Test specimens were fabricated using the hand winding method with phenol-formaldehyde resin as the binder and four types of reinforcing fabrics: carbon, basalt, glass, and silica. A comprehensive set of tests was conducted, including tensile strength (up to 420 MPa), compressive strength (up to 310 MPa), Brinell hardness (ranging from 29 to 43 HB), thermal conductivity (from 0.045 to 0.39 W/(m·K)), and thermal resistance under direct high-temperature gas exposure (rear surface temperatures from ~250 to 350 °C). The results demonstrated that composites reinforced with carbon fabric exhibited the highest mechanical strength and heat resistance, whereas silica-based composites showed the lowest thermal conductivity and the best thermal insulation performance, making them suitable for internal thermal protection of combustion chambers and nozzles in rocket propulsion systems.**

***Keywords:*** High-temperature composites, Phenol-formaldehyde resin, Reinforcing fibers, Filament winding method, Thermal insulation materials, Mechanical testing, Fire testing, Thermal conductivity

## 1. Introduction

During the operation of a solid rocket motor (SRM), the combustion chamber is subjected to extremely high temperatures and significant mechanical loads. Under such conditions, the implementation of a thermal protection system (TPS) becomes a critical component of the design. Fig. 1 presents a simplified schematic of an SRM combustion chamber, indicating the propellant grain, thermal barrier, thermal insulation, and casing [1,2].

Fiber-reinforced composite materials are widely used in the aerospace industry due to their combination of high thermal resistance and mechanical strength. To enhance thermal protection performance, various combinations of matrix and reinforcing filler are being investigated [3—5].

The study presented in Ref. [6] investigated glass and carbon fiber composites based on polyester resin, fabricated using the filament winding method. The results showed that hybrid reinforced structures demonstrated improved thermal resistance (up to 192 s at 3000 °C).

The study presented in Ref. [7] investigated the strength and deformation behavior of a composite material based on an epoxy matrix reinforced with fiberglass fabric. The flexural strength reached up to 178 MPa, the compressive modulus of elasticity up to 13 GPa, and the elongation at break was in the range of 0.6—0.8 %. In Ref. [8], the strength characteristics of multilayer composites based on basalt and glass fabrics with an epoxy matrix were investigated, including finite element modeling. The results showed that the use of basalt fabric without glass mat increases the

Received 2 July 2025; revised 10 October 2025; accepted 14 October 2025.
Available online 20 November 2025

* Corresponding author at: Faculty of Mechanics and Mathematics, Al-Farabi Kazakh National University, Almaty 050040, Kazakhstan.
E-mail address: m.sadykov@spaceres.kz (M.Sh. Sadykov).

*https://doi.org/10.69912/2616-8537.1263*

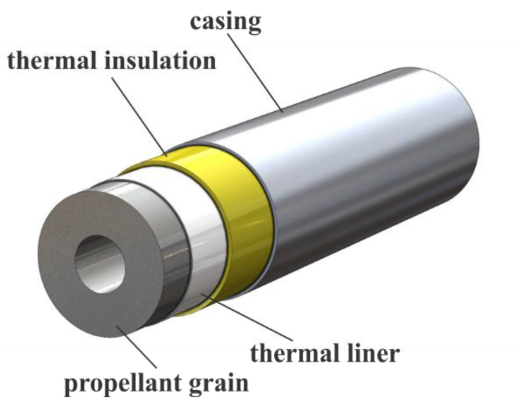


*Fig. 1. SRM combustion chamber.*

material's strength and reduces the risk of interlayer failure. In Ref. [9], the effects of various matrix systems-epoxy, bismaleimide, and cyanate ester resins - on the mechanical, thermal, and electrical properties of carbon fiber reinforced composites were studied. It was established that the choice of matrix has a significant impact on the strength, thermal conductivity, and dielectric properties of the composites, with cyanate ester-based materials demonstrating the highest thermal stability and electrical insulation performance.

In study [10], the thermal insulation properties of multilayer composite materials based on epoxy and phenol-formaldehyde (PF) resins with various types of reinforcement - including glass fiber, basalt fiber, ceramic and wrapping paper - were investigated. The primary focus was on measuring thermal diffusivity using the laser flash method in the temperature range of 50–200 °C. The results showed that the best thermal insulation performance was demonstrated by the composite based on epoxy resin EPOLAM 2025 reinforced with ceramic paper, which achieved the lowest thermal diffusivity value of 0.074 $mm^2/s$ at 200 °C. All tested composites exhibited satisfactory characteristics suitable for use in solid-propellant rocket motor structures.

The binder systems, which ensure the structural integrity and thermal resistance of the composites, play an equally critical role. Although PF resins have a limited operational temperature (~250 °C), they are capable of forming a carbonaceous char upon thermal exposure, which remains stable at temperatures up to 2000 °C in an inert atmosphere [11]. Chapter [12] of the reference book provides a detailed analysis of the differences between resols and novolacs. Resols are synthesized in an alkaline medium with an excess of formaldehyde and are capable of curing without additional agents, whereas novolacs require hexamethylenetetramine for crosslinking. In Ref. [13], the dynamic mechanical properties of resol-type phenolic resins under various curing conditions were examined. Dynamic mechanical analysis was used to determine optimal temperature ranges for gelation (98–129 °C) and condensation (139–151 °C). Increasing the curing temperature resulted in more complete polycondensation and reduced residual flow behavior.

Thus, PF resins form a heat-resistant carbonaceous matrix upon heating, making them ideal for components exposed to extreme thermal environments. The microstructure, fiber winding angles, and curing regime control are critical factors influencing the thermal performance of the resulting composites.

A key stage in the fabrication of such materials is the structuring technology. Unlike pressing or infiltration methods, hand filament winding enables the formation of cylindrical or axisymmetric preforms with controlled fiber orientation, uniform wall thickness, and high reproducibility of shape. Particular interest lies in the production of tubular structures, as they serve as fundamental elements for internal thermal protection in combustion chambers, pre-chambers, nozzles, and other components exposed to high-temperature gas flows. This geometry ensures not only optimal load and heat distribution but also allows the composite tube to function as a liner or inner insulation layer in multilayer thermal protection systems [14–17].

As a result of the analysis of scientific literature, optimal starting materials with high performance characteristics were selected to address the stated research objectives. Among the most promising reinforcing components, special attention was given to carbon, silica, basalt, and fiberglass materials due to their low density, high strength, and corrosion resistance. Based on the literature review, PF resin was chosen as the binder, providing a necessary balance between mechanical strength, thermal resistance, and adhesion properties.

The objective of this study is to investigate fabrication technologies for composite thermal insulation materials using the filament winding method with various types of reinforcing fibers. The study focuses on evaluating the mechanical and thermal properties of the resulting specimens, including tensile and compressive strength, fire resistance, and thermal conductivity.

## 2. Material and methods (experimental or methodology or patients and methods)

### *2.1. Materials*

In this study, various technical fabrics with different properties were used as reinforcing fillers: carbon fabric (twill weave, 180 $g/m^2$, JSC “UMATEX”, Russia), silica fabric (300 $g/m^2$, Changshu Jiangnan Glass Fiber

Co., Ltd., China), basalt fabric TBK-100 (210 g/m$^2$, Polotsk-Steklovolokno, Belarus), and glass fabrics ("Armplast", Russia).

As a binder, a phenol-formaldehyde (PF) resin of grade R-75, manufactured by Shandong Shengquan Group Co., Ltd. (Jinan, China), was employed. This resin belongs to the resol-type thermosetting binders, which are capable of curing without the addition of external hardeners, thereby simplifying the production process. The properties of the PF resin used in this study are summarized in Table 1.

One of the key advantages of this resin is its ability to form a carbonaceous char upon heating, which remains stable at temperatures up to 2000 °C in an inert atmosphere. Owing to these properties, R-75 PF resin is highly effective in the fabrication of thermal protection composites for rocket and aerospace applications, particularly under conditions involving ablation and high-temperature gas exposure.

### 2.2. Fabrication process (filament winding method)

Based on the selected materials, specimens of high-temperature thermal insulation materials (HTIMs) were fabricated using the hand filament winding method. Four types of reinforcing fabrics were used in the study: carbon, silica, basalt, and glass; PF resin served as the binder.

In the first stage, component preparation was carried out. A custom-designed mandrel, specifically developed for this fabrication method, was used as the winding base (Fig. 2).

The forming tool consists of a cylindrical structure made from a steel billet. The internal diameter of the mandrel is 25 mm, and the working length is 300 mm, corresponding to the inner diameter of the molded specimens. Taking into account the thickness of the reinforcing material winding (4 mm), the outer diameter of the sample after forming is 33 mm.

The tool includes a split forming shell composed of two semi-cylindrical parts. This shell is designed to enclose the wound preform and provide uniform pressure on its surface during thermal treatment. The two-part design simplifies assembly and disassembly and reduces the risk of sample damage during demolding after curing.

To ensure external shell fixation and stabilize the geometry, three metal clamps were used, evenly distributed along the length of the mandrel. Their main functions are as follows:

- To provide uniform compression of the reinforcing layers and secure the winding during forming;
- To maintain the cylindrical shape of the preform during thermal treatment, including compensation for possible thermal deformation;
- To reduce the risk of internal stresses and local fabric bulging by stabilizing the outer shell.

The combined use of a split shell and clamps ensures geometric stability, structural uniformity, and

*Table 1. Main characteristics and advantages of R-75 PF resin.*

| Parameter | Value/Description |
|---|---|
| Resin type | Resol-type phenol-formaldehyde resin |
| Maximum operating temperature, °C | Up to 250 |
| Viscosity at 25 °C, mPa·s | 2500—3500 |
| Thermal stability after carbonization, °C | Up to 2000 (in inert atmosphere) |

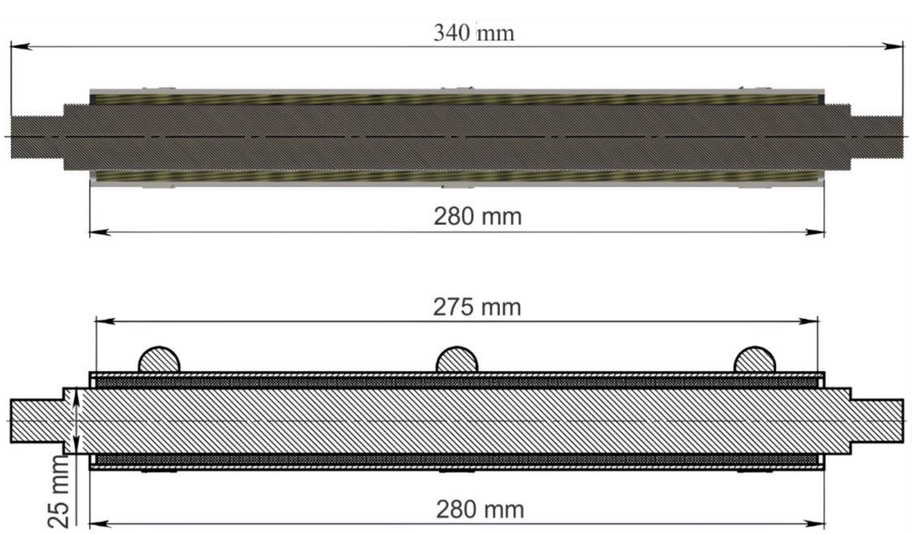


*Fig. 2. Design drawing of the forming tool (HTIMs).*

reproducibility of the fabricated samples, which is critical for reliable mechanical and thermal testing.

In the second stage, the actual winding of the reinforcing fabric layers onto the prepared mandrel was carried out. The fabrics were cut into strips 270 mm wide, with lengths varying depending on the areal density of the material to achieve a wall thickness of 4 mm. The PF resin was prepared according to technical specifications. Before application, the viscosity was checked, and the resin was thoroughly mixed to obtain a homogeneous composition.

The fabric strips were pre-impregnated with PF resin to ensure uniform resin distribution. The layers were manually laid with consistent tension, allowing the formation of the specified total wall thickness (~4 mm). The fabric was impregnated by hand with even distribution across the entire surface, followed by dense and uniform manual winding onto the mandrel with careful alignment of each layer. A pressing roller was used to prevent air entrapment.

Carbon and silica fabrics had a nominal thickness of 0.31 mm; to achieve the desired preform thickness, strips were cut to a length of 700 mm. Basalt and glass fabrics had a lower thickness of 0.18 mm, so their strip length was increased to 1000 mm. This approach ensured uniform wall thickness and comparability of the obtained samples, which is essential for accurate analysis of their physical, mechanical, and thermal properties.

The outer shell and clamps maintained the necessary form and winding density before and during curing. The fabrication process consisted of several sequential stages (Fig. 3).

In the third stage, the specimens underwent heat treatment to cure the binder. The wound assembly (together with the outer shell) was placed into a heating furnace and subjected to a two-step temperature regime. Initially, preheating was performed at 120 °C for 30 min, followed by cooling to room temperature (~30 min). Final curing was then carried out at 150 °C for 1 h, followed by cooling for no less than 30 min. This regime enabled gradual polymerization of the PF resin, preventing rapid release of volatiles and the formation of internal stresses within the material.

After completing the full heat treatment and cooling cycle, the HTIM component was formed. The metal clamps were removed, the split outer shell was disassembled, and the internal mandrel was easily extracted from the composite tube thanks to the use of a paper release layer, which prevented damage to the structure. The resulting product was a cylindrical sample of fiber-reinforced thermal insulation material with an inner diameter of approximately 25 mm (equal to the mandrel diameter), a wall thickness of ~4 mm, and an outer diameter of ~29 mm. The length of the cured specimen was 275 mm, with slight variations possible due to thermal processing.

As a result of the winding and curing process, robust tubular preforms were obtained, fully prepared for testing. The fabricated composites were subsequently subjected to mechanical evaluation, including compressive and tensile strength testing, flame

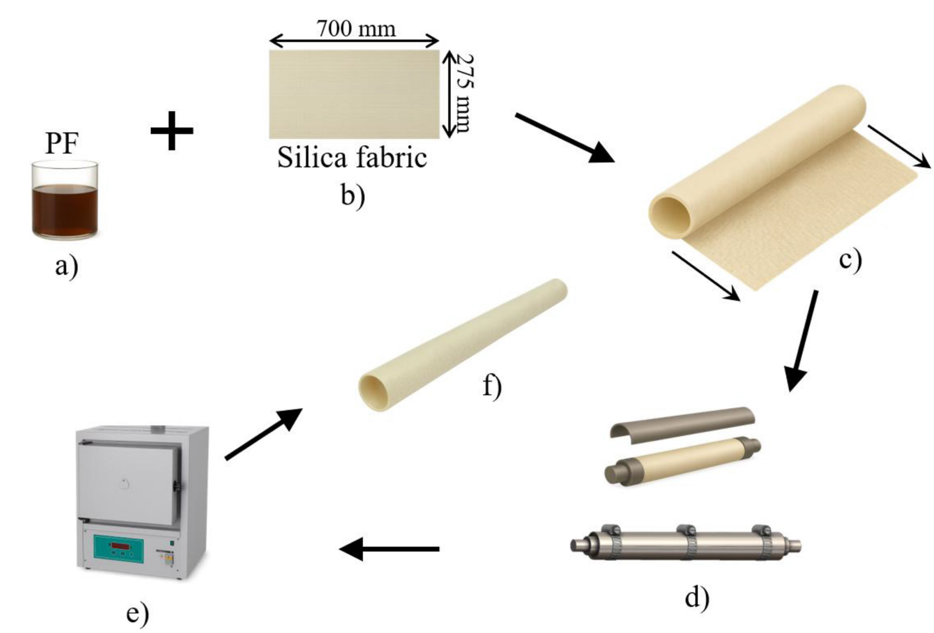


*Fig. 3. Schematic representation of the composite fabrication process: (a) preparation of PF resin, (b) preparation of the reinforcement material (silica fabric), (c) impregnation with binder, (d) material forming, (e) curing, (f) final specimen.*

resistance assessments, and thermal conductivity measurements.

This method ensured a high degree of impregnation of the reinforcing fabrics and the formation of a uniform composite structure. The resulting specimens are intended for further investigation of their thermal resistance, mechanical strength, and other performance characteristics within the framework of a development program for thermal protection coatings for aerospace components.

### *2.3. Test methods*

#### *2.3.1. Tensile and compression testing*

The mechanical properties of the composite materials under investigation were evaluated through tensile and compression testing in accordance with ASTM D3039 and ASTM D5449 standards [18,19]. A universal testing machine (RMG-100MG4) was used for all experiments. The composite tube specimens were fabricated and prepared following the requirements of the specified standards. Each specimen was mounted in the grips of the testing machine according to the established procedures.

During tensile testing, the load was applied uniformly, and the crosshead displacement rate was maintained at 0.2 MPa/s until specimen failure, allowing for the determination of ultimate tensile strength. Similarly, during compression testing, the critical load at which local plastic deformation and subsequent failure began was recorded.

All tests were conducted under standard laboratory conditions (temperature 23 ± 2 °C, relative humidity 50 ± 5 %). For each composite configuration, a series of five tests was performed, and the results were averaged to improve the reliability of the obtained data.

#### *2.3.2. Hardness testing*

Hardness measurements of the composite plate specimens were performed using a Brinell hardness tester (TP5014-01). The tests were carried out by indenting a 10 mm diameter steel ball into the sample surface under a load of 500 kgf, with a dwell time of 10 s. After the load was removed, the diameter of the indentation was measured, and the Brinell hardness (HB) was calculated in accordance with the procedure specified in GOST 4670-2015 [20]. Prior to testing, the specimen surfaces were ground to ensure uniform testing conditions and to minimize the influence of surface defects.

#### *2.3.3. Fire resistance testing of materials*

The thermal resistance of the composite materials was evaluated using a test bench equipped with a propane—oxygen torch, producing a flame temperature of approximately 2000 °C, in accordance with the principles of ISO 2685 and ASTM E84 standards [21,22]. The samples were prepared in the form of flat plates and mounted so that their front surface was directly exposed to the flame until the onset of material failure. The rear-surface temperature was continuously recorded in real time using a UNI-T thermal imaging camera. The exposure time varied depending on the composite type, ranging from ~15 to 47 s. After exposure, the temperature on the rear surface was recorded in real time using a UNI-T thermal imaging camera (Fig. 4).

The evaluation criteria for fire resistance included:

(i) the maximum rear-surface temperature reached before failure,
(ii) the time to material failure (structural collapse, burning-through, or delamination), and
(iii) the ability of the material to maintain structural integrity during flame exposure.

The resulting temperature curves were used to assess the thermal protection efficiency of composites with various types of reinforcing fillers and resins. Key evaluation criteria included: the minimum temperature recorded on the rear surface, the rate of temperature increase, and the ability of the material to maintain structural integrity under intense thermal exposure.

All tests were carried out under standard laboratory conditions (temperature 23 ± 2 °C, relative humidity 50 ± 5 %). For each composite configuration, a series of five tests was performed, and the results were averaged to enhance the reliability of the obtained data.

#### *2.3.4. Thermal conductivity measurement*

The thermal conductivity of the composite specimens was measured using a DRP-II thermal conductivity analyzer, in accordance with the principles of ASTM C177-19 [23]. The measurement method was based on recording the heat flux and temperature difference under a defined thermal regime. The samples were prepared in the form of flat plates and positioned between the heating and cooling elements of the device, allowing for the establishment of a steady-state or quasi-steady-state thermal field. The instrument automatically calculated the thermal conductivity coefficient ($\lambda$) using the measured temperature gradient, sample thickness, and heat flux (Fig. 5).

All tests were conducted under standard laboratory conditions (temperature 23 ± 2 °C, relative humidity 50 ± 5 %). For each composite configuration, a series of five tests was performed, and the results were

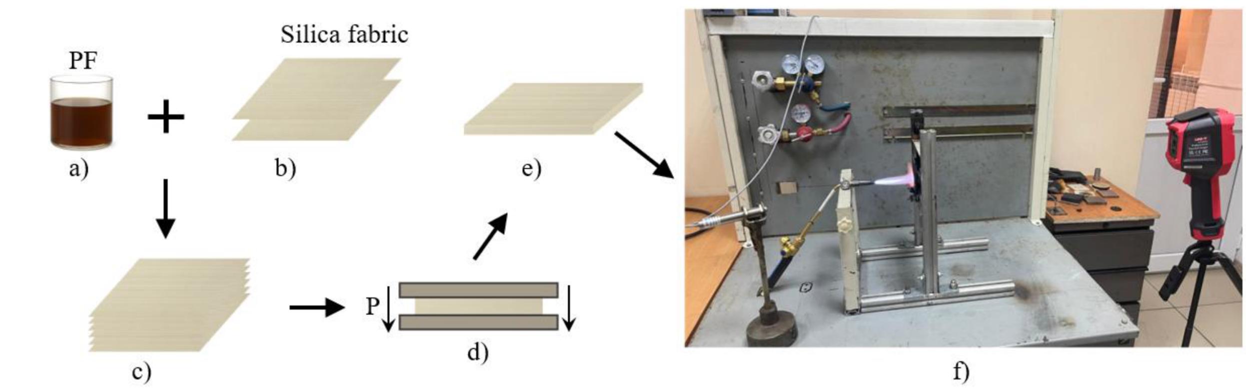


*Fig. 4. Technological process for producing HTIMs and setup for fire resistance testing: (a) PF resin preparation, (b) reinforcement preparation, (c) impregnation with binder, (d) pressing, (e) final specimen, (f) test bench with propane-oxygen torch and thermal imager.*

averaged to improve the reliability of the obtained data.

## 3. Results and discussion

### *3.1. Mechanical testing*

Fig. 6 presents a comparison of the compressive and tensile strength properties (in MPa) of four types of reinforcing fabrics. Compressive and tensile strength values are shown on the left (blue) and right (red) y-axes, respectively. The highest performance was demonstrated by the carbon fabric, with compressive strength of 310 MPa and tensile strength of 420 MPa. These values exceed those of the silica fabric, which exhibited the lowest properties, by more than three times: 101 MPa in compression and 164 MPa in tension. The basalt fabric showed intermediate values, with 210 MPa in compression and 270 MPa in tension, approximately twice as high as those of the silica

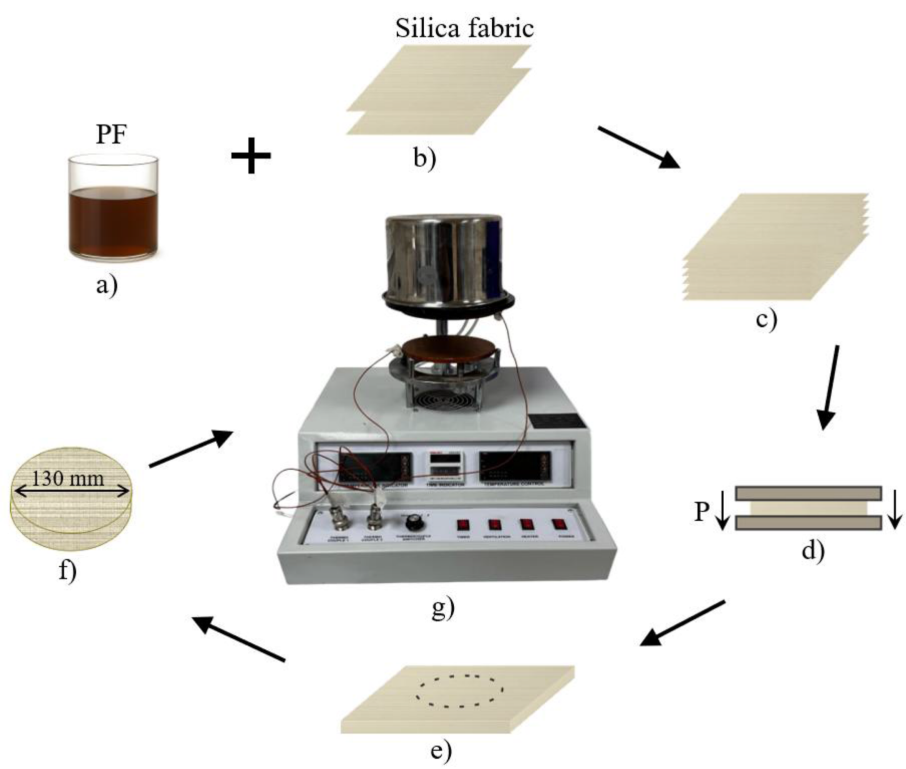


*Fig. 5. Technological process for producing HTIMs for thermal conductivity measurement: (a) resin preparation, (b) reinforcement preparation, (c) impregnation with binder, (d) pressing, (e) cutting the specimen from the cured laminate with defined geometry, (f) final specimen, (g) DRP-II thermal conductivity analyzer.*

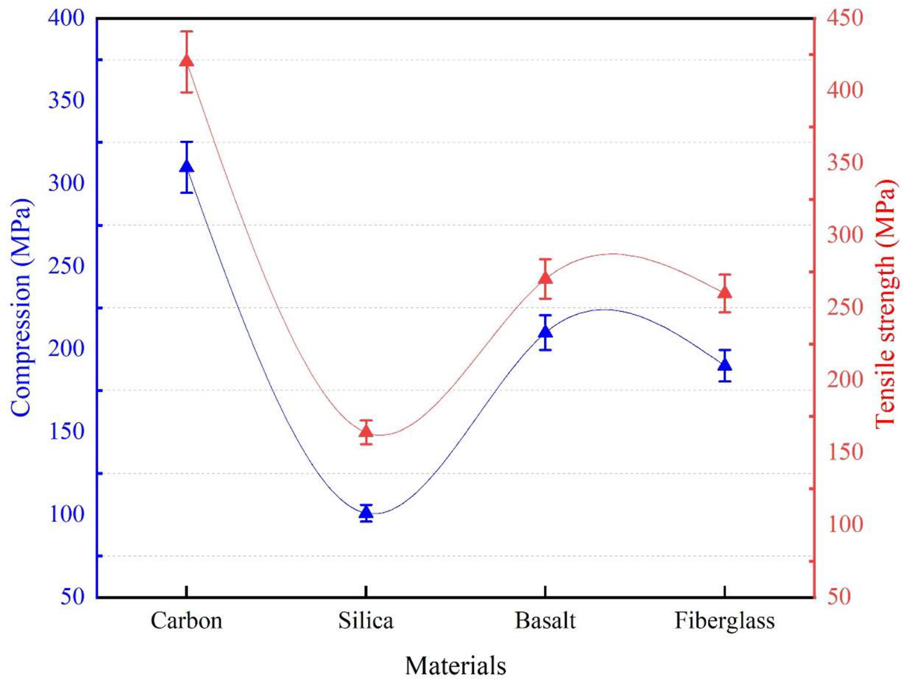


*Fig. 6. Compression and tensile test results.*

fabric. The glass fabric also demonstrated respectable properties - 190 MPa in compression and 260 MPa in tension - slightly lower than basalt but significantly surpassing silica.

The presented data clearly demonstrate significant differences in the mechanical properties of the fabrics, highlighting the necessity of a reasoned selection based on the operating conditions of the structure.

Fig. 7 shows the Brinell hardness test results for specimens reinforced with different types of fabrics. The bar chart illustrates the comparative hardness levels, accompanied by error bars indicated in red.

The highest hardness value was recorded for the carbon fabric-approximately 43 HB-highlighting its high mechanical strength and resistance to indentation. The basalt fabric exhibited a hardness of about 35 HB, approximately 19 % lower than carbon but surpassing silica and glass fabrics. The silica fabric reached approximately 31 HB, while the glass fabric showed the lowest value at about 29 HB, roughly 33 % lower than carbon.

Thus, the hardness of the material also varies depending on the type of reinforcing filler. Carbon and basalt fabrics provide higher resistance to mechanical damage, making them preferable for applications involving abrasive or impact loads.

### *3.2. Thermal testing*

Fig. 8 presents the results of flame resistance tests, reflecting the thermal stability of various reinforcing fabrics based on the maximum temperature reached during thermal exposure. The values are accompanied by error bars indicated by vertical lines.

The highest thermal resistance was demonstrated by the silica fabric, which reached temperatures of approximately 350 °C, confirming its gradual and stable heating behavior under flame exposure. Carbon, basalt, and fiberglass fabrics exhibited similar maximum values-around 250—300 °C-before a sharp

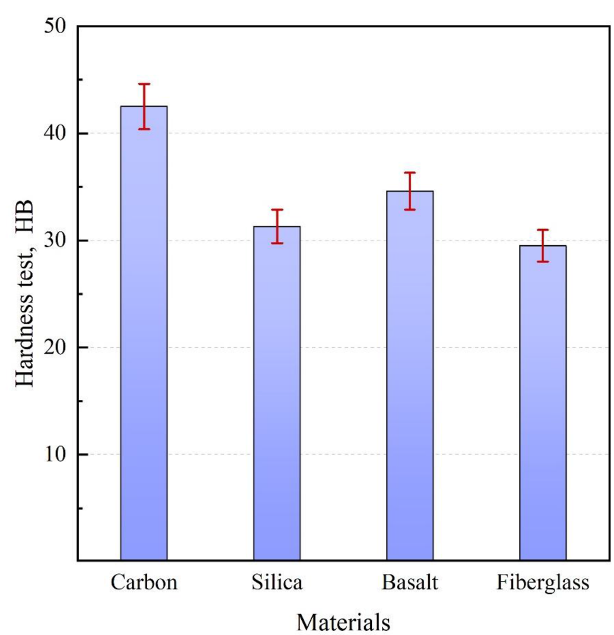


*Fig. 7. Hardness test results.*

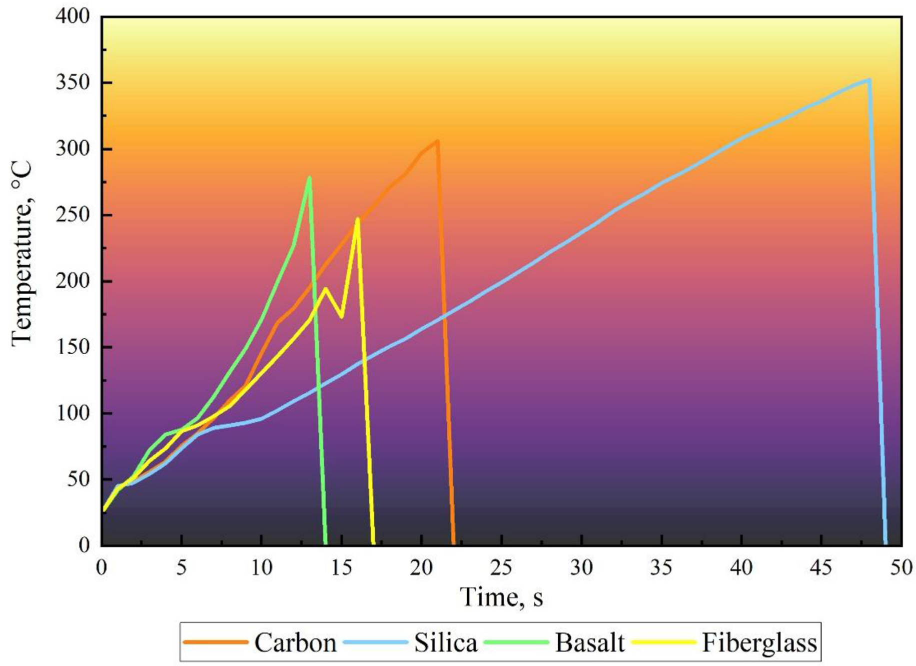


*Fig. 8. Flame resistance test results.*

temperature drop, indicating their faster degradation or burning onset. These results confirm that the choice of reinforcing material significantly influences the thermal stability of the composite structure, which is especially important when designing thermal protection systems for high-temperature zones such as combustion chambers and rocket nozzles.

Fig. 9 presents the thermal conductivity measurements (W/(m·K)) of various types of reinforcing fabrics. The data are visualized as a curve showing the dependence of the thermal conductivity coefficient on the material type.

The highest thermal conductivity was recorded for the carbon material, at approximately 0.39 W/(m·K). This value is nearly nine times greater than that of the silica material, which exhibited the lowest conductivity of 0.045 W/(m·K). This sharp contrast highlights the pronounced insulating properties of the silica fabric and the high thermal conductivity of the carbon reinforcing component.

The basalt material showed a thermal conductivity of about 0.14 W/(m·K), roughly three times higher than that of silica but 2.8 times lower than carbon. The glass fabric demonstrated a value of approximately

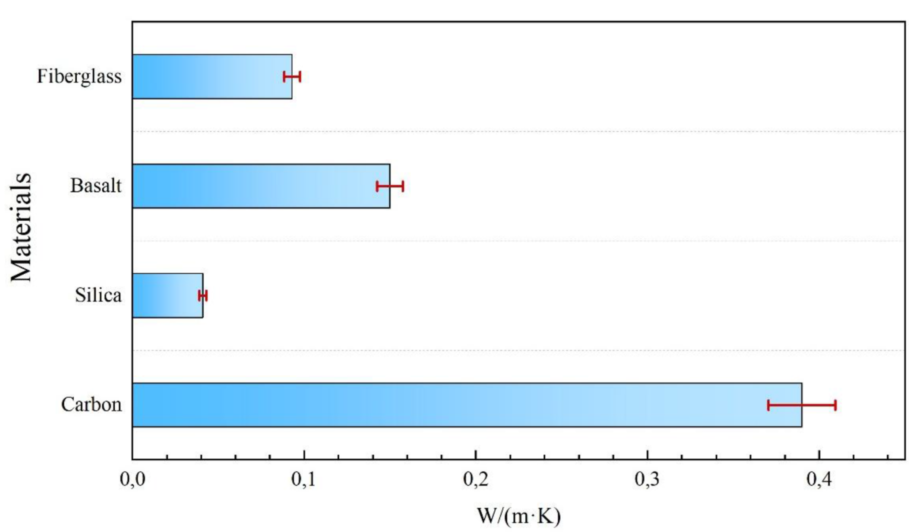


*Fig. 9. Thermal conductivity test results.*

*Table 2. Mechanical and thermal properties of composite materials based on phenol–formaldehyde resin (mean ± SD).*

| Composite type | Tensile strength (MPa) | Compressive strength (MPa) | Hardness Test (HB) | Thermal conductivity (W/(m·K)) | Flame resistance (max °C) |
|---|---|---|---|---|---|
| Carbon fabric | 420 (±21) | 310 (±15.5) | 42.5 (±2.13) | 0.39 (±0.02) | 300 (±16) |
| Silica fabric | 164 (±8.2) | 101 (±5.05) | 31.3 (±1.57) | 0.041 (±0.002) | 350 (±16) |
| Basalt fabric | 270 (±13.5) | 210 (±10.5) | 34.6 (±1.73) | 0.15 (±0.007) | 280 (±16) |
| Fiberglass | 260 (±13) | 190 (±9.5) | 29.5 (±1.48) | 0.093 (±0.004) | 270 (±16) |

0.09 W/(m·K)-100 % higher than silica but nearly 77 % lower than carbon.

Thus, the range of thermal conductivity among the studied materials varies by more than an order of magnitude. This emphasizes the necessity of careful selection of the reinforcing component depending on the required thermal performance of the composite material.

Table 2 presents the averaged mechanical and thermal characteristics of the studied composites, including strength properties, hardness, thermal conductivity, and maximum flame resistance. The summarized data provide a clear comparison of the materials and help identify the most suitable option for operation under high load and temperature conditions.

## 4. Conclusion

The conducted study demonstrated the effectiveness of the hand filament winding technology for fabricating high-temperature insulation composites based on phenol-formaldehyde resin and various types of reinforcing fabrics. The produced cylindrical preforms exhibited stable geometry, uniform structure, and reproducible wall thickness, ensuring reliability during thermal and mechanical testing.

Based on the quantitative data, composites with carbon fabric possess the best strength (up to 420 MPa in tensile strength), hardness (43 HB), and the highest thermal conductivity (0.39 W/(m·K)). Basalt fabric and fiberglass composites provided a balanced combination of mechanical and thermal properties. Composites with silica fabric showed the lowest strength, but exhibited the best thermal insulation performance ($\lambda \approx 0.045$ W/(m·K)) and the most stable behavior under short-term flame exposure, the maintaining structural integrity up to 350 °C. These results enable informed selection of reinforcing materials according to prioritized operational requirements.

## Funding

This research has been funded by the Science Committee of the Ministry of Science and Higher Education of the Republic of Kazakhstan (grant No. AP234038/0223).

## Conflicts of interest

The authors declare that they have no competing interests.

## References

[1] A. Mahjub, N.M. Mazlan, M.Z. Abdullah, Q. Azam, Design optimization of solid rocket propulsion: a survey of recent advancements, J. Spacecr. Rockets 57 (2020) 3–11.
[2] O. Uyanna, H. Najafi, Thermal protection systems for space vehicles: a review on technology development, current challenges and future prospects, Acta Astronaut. 176 (2020) 341–356.
[3] M. Meiirbekov, A. Kuandyk, M. Sadykov, M. Nurzhanov, N. Yesbolov, B. Baiserikov, et al., Polymer-based thermal protective composites: the role of reinforcement and matrix in providing strength and fire resistance, Polymers (Basel) 17 (2025) 1419.
[4] Y. Hirai, H. Hamada, J.-K. Kim, Impact response of woven glass-fabric composites—I, Compos. Sci. Technol. 58 (1998) 91–104.
[5] Pareek K, Saha P. Basalt fiber and its composites: an overview [Internet]. Available from: https://www.researchgate.net/publication/331982825.
[6] J. Rusmirović, J. Galović, M. Kluz, S. Perković, S. Brzić, M. Bogosavljević, et al., Using potential of filament-wound carbon/glass polymeric composites as rocket motor thermal insulation, Polym. Polym. Compos. 29 (2021) S1541–S1554.
[7] E.V. Filimonov, N.V. Linkov, Strength and Deformation Behavior of a Composite Material Based on an Epoxy Matrix and Fiberglass Fabric, 2010. Moscow.
[8] A. Karnoub, D.B. Nezhizhimov, K.S. Shirinyan, Research and modeling of a multilayer composite material using basalt fabric, Vestnik Don State Tec. Univ. 20 (2020) 5–14.
[9] D. Wang, S. Hu, J. Vecernik, D. Kremenakova, J. Militky, J. Novotna, Impact of different matrix systems on mechanical, thermal, and electrical properties of carbon fiber reinforced epoxy resin matrix composites, Polym. Compos. 45 (2024) 12225–12237.
[10] A. Dominiak, M. Rąpała, R. Domański, B. Bartkowiak, P. Darnowski, Solid-fuel rocket engines: layered composite materials manufacturing and thermal diffusivity measurements, High Temp. Mater. Process. 33 (2014) 171–177.
[11] X. Wang, Q. Xu, Q. Zheng, Y. Shao, J. Shen, Reviews of fiber-reinforced phenolic resin-based thermal protection materials for aircraft, Energies (Basel) 18 (2025) 819.
[12] A. Pizzi, C.C. Ibeh, Phenol–Formaldehydes. Handbook of Thermoset Plastics, Elsevier, 2014, pp. 13–44.
[13] R.A. Haupt, TJr Sellers, Characterizations of phenol-formaldehyde resol resins, Ind. Eng. Chem. Res. 33 (1994) 693–697.
[14] I.I. Karpovich, Y.S. Myhovych, Selection of mandrel type for winding rocket engine casings, Sys. Design Analysis Aero. Tech. Charact. 32 (2023) 61–71.
[15] A.J. Lauder, Manufacture of rocket motor cases using advanced filament winding processes, Mater. Manuf. Process. 10 (1995) 75–87.
[16] X. He, Y. Shi, C. Kang, T. Yu, Analysis and control of the compaction force in the composite prepreg tape winding process for rocket motor nozzles, Chin. J. Aeronaut. 30 (2017) 836–845.
[17] M. Meiirbekov, A. Yermekov, M. Nurguzhin, A. Kulbekov, Identifying the influence of winding angles on the strength

properties of carbon fiber-reinforced plastic tubes, E. Eur. J. Enterprise Technol. 1 (2025) 26—32.
[18] ASTM International, ASTM D3039/D3039M-17: Standard Test Method for Tensile Properties of Polymer Matrix Composite Materials, ASTM International, West Conshohocken (PA), 2017.
[19] ASTM International. ASTM D5449-02, Standard Test Method for Compressive Properties of Unidirectional Polymer Matrix Composite Tubes, ASTM International, West Conshohocken (PA), 2017, 2017.
[20] Federal Agency on Technical Regulating and Metrology, GOST 4670-2015: Plastics — Determination of Hardness by Ball Indentation Method, Standartinform, Moscow, 2016.
[21] International Organization for Standardization, ISO 2685:1998: Aircraft — Environmental Test Procedures for Airborne Equipment — Resistance to Fire in Designated Fire Zones, ISO, Geneva, 1998.
[22] ASTM International, ASTM E84-23: Standard Test Method for Surface Burning Characteristics of Building Materials, ASTM International, West Conshohocken (PA), 2023.
[23] ASTM International, ASTM C177-19: Standard Test Method for Steady-State Heat Flux Measurements and Thermal Transmission Properties by Means of the Guarded-Hot-Plate Apparatus, ASTM International, West Conshohocken (PA), 2019.